

# Corrosion behaviour of silicon carbide particle reinforced 6061/Al alloy composites

M. S. N. BHAT, M. K. SURAPPA

*Department of Metallurgy, Indian Institute of Science, Bangalore 560012, India*

H. V. SUDHAKER NAYAK

*Department of Metallurgical Engineering, Karnataka Regional Engineering College, Srinivasanagar, Surathkal 574157, India*

The corrosion behaviour of 6061 Al alloy–SiC<sub>p</sub> composites (in as cast and extruded form) have been studied in sea water and acid media. The effects of temperature of both the media and concentration of the acid medium were also investigated. The corrosion behaviour was evaluated using electrochemical technique and corroded specimens were examined using scanning electron microscopy. The studies revealed that corrosion damage of composites exposed to sea water medium was mainly localized in contrast to uniform corrosion observed for base alloy. Further, composites were found to corrode faster than the base alloy even though the attack was mainly confined to the interface, resulting in crevices or pits. This could be attributed to the presence of thin layer of reaction product present at the interface acting as an effective cathode which when continuous would increase the cathode to anode ratio enabling higher localized corrosion. However, the extent of corrosion damage in extruded composites was less possibly due to absence of defects like gas pores in the composites and homogeneity in the distribution of particles. Increase in temperature invariably increased the attack for all the materials studied. This is explained due to the metal dissolution (anodic process) which is governed by the kinetics at that temperature.

## 1. Introduction

Aluminium matrix composites find extensive applications because of their high strength to weight ratio, high specific modulus and unique combination of several tailored properties. These engineered composites consist of continuous or discontinuous fibres, whiskers or particulates in the aluminium alloy matrix. Extensive investigations on the production, characterization and corrosion behaviour of aluminium matrix composites reinforced with carbon, graphite, boron, alumina and silicon carbide fibres have been carried out. Their mechanical, physical and tribological properties were well documented [1, 2]. Similarly discontinuously reinforced aluminium matrix composites containing particles, whiskers or short fibers of SiC or Al<sub>2</sub>O<sub>3</sub> have been studied [2, 3] for their physical and mechanical properties. However, not much information is available on the corrosion behaviour of discontinuously reinforced Al matrix composites.

Aluminium alloy/graphite composites were found to be more susceptible to corrosion in marine environment than the base alloy [4], probably due to galvanic effects caused by the formation of aluminium carbide (Al<sub>4</sub>C<sub>3</sub>) at the interface between graphite and aluminium. However, no such galvanic effect is observed in the case of Al–Si alloy/graphite composites in sea water medium. Boron fibre reinforced 2024 Al and 6061 Al alloy showed crevice corrosion at the interface

because of the rupture of passive film and increase in anodic sites. Presence of aluminium boride at the interface enhanced galvanic corrosion [5]. The increase in volume fraction of Boron fibre shifted the corrosion potential towards more negative values [6]. It was found that [1, 7] Al–SiC<sub>f</sub> corrode at slower rate in marine environment than Al/graphite composites. On the other hand, these composites have higher rate of corrosion and suffer localized damage when compared to their matrix alloys. Corrosion characteristics of Al alloy/mica particulate composites [8] in de-aerated 3.5% NaCl were also reported and the composites were found to have higher corrosion rates than the matrix alloys. This was explained on the basis of a discontinuous film providing sites for pitting and crevice corrosion. Studies [9] on the corrosion behaviour of 2024 Al/SiC<sub>w</sub> showed less effect of SiC phase on the resistance to pit initiation.

In the present investigation an attempt is made to evaluate the corrosion behaviour of 6061 Al/SiC<sub>p</sub> composites in as cast and extruded conditions, both in H<sub>2</sub>SO<sub>4</sub> and sea water media. Effects of acid concentration and temperature are also studied. For the purpose of comparison, corrosion behaviour of base alloy (6061 Al) is also studied.

## 2. Experimental procedure

Composites containing 15 wt % SiC particles of approximately 40 μm size were prepared by vortex

TABLE I Chemical composition of base metal and reinforcements  
(A) Base metal

Element	Cu	Mg	Si	Cr	Al
Wt %	0.25	1.0	0.6	0.25	Bal

(B) Reinforcement

Constituent	SiC	SiO <sub>2</sub>	C	Al <sub>2</sub> O <sub>3</sub>	Si	Fe <sub>2</sub> O <sub>3</sub>
Wt %	98.8	0.75	0.4	0.20	0.60	0.05

method [10] and extruded after solutionising for 3 h at 775 K.

The chemical composition of the base alloy and reinforcement used are given in Table I.

The corrosion studies were carried out in 1 N, 2 N, 3 N H<sub>2</sub>SO<sub>4</sub> solution and natural sea water at 300 and 325 K. The composition of sea water is given in Table II.

Circular coupons of 15 mm dia. were cut from all the materials (base alloy, cast and extruded composites). These specimens were wet polished with SiC papers to 5/0 grit level and later disc polished using diamond paste (< 2 μm size). The steady state open-circuit potentials (measured against a saturated calomel electrode) were obtained from potential-time measurements. The general corrosion behaviour of these materials at two different temperatures of the media (controlled to ± 2° accuracy) were evaluated by electro-chemical measurements using a Wenking model POS-73 Potentiostat. Cathodic and anodic polarization were made with a potential scan rate of 50 mV min<sup>-1</sup>. JEOL 840A scanning electron microscope was used to study the corroded surface after anodic polarization.

### 3. Results

The steady-state open circuit potentials (o.c.p.) for various systems are given in Table III. The o.c.p.s of composites and base alloy shift to more negative values as the temperature and concentration of the media increase. The potentiodynamic polarization curves for different systems studied are given in Figs 1a, b and 2a-c. The corrosion rates as computed from Tafel extrapolation technique (Table IV) indicate that the composites in the extruded form always have a lower corrosion rate as compared to base alloy especially at higher concentration of acid.

Fig. 3a-c are the SEM photomicrographs of corroded surfaces of samples anodically polarized in sea water at 300 K. It can be seen while the attack is uniform and is very severe in the base alloy, it is comparatively less and localized in the case of extruded composites. Although, as cast composites show higher attack it is around the particles and the pores. The SEM photomicrographs for 3 N H<sub>2</sub>SO<sub>4</sub> medium

TABLE III Steady state open circuit potentials (o.c.p.)

Material	Open circuit potential (V)			
	Sea water 1 N	2 N	3 N	
	H <sub>2</sub> SO <sub>4</sub>	H <sub>2</sub> SO <sub>4</sub>	H <sub>2</sub> SO <sub>4</sub>	
<i>A. Base alloy (6061 Al)</i>				
Temp. 300K	-0.750	-0.640	-0.660	-0.660
325K	-0.755	-0.700	-0.720	-0.750
<i>B. Composite (6061 Al-15 Wt % SiC<sub>p</sub>)</i>				
(i) As cast				
Temp. 300K	-0.810	-0.650	-0.660	-0.690
325K	-0.820	-0.690	-0.710	-0.730
(ii) Extruded				
Temp. 300K	-0.790	-0.700	-0.710	-0.740
325K	-0.830	-0.710	-0.720	-0.760

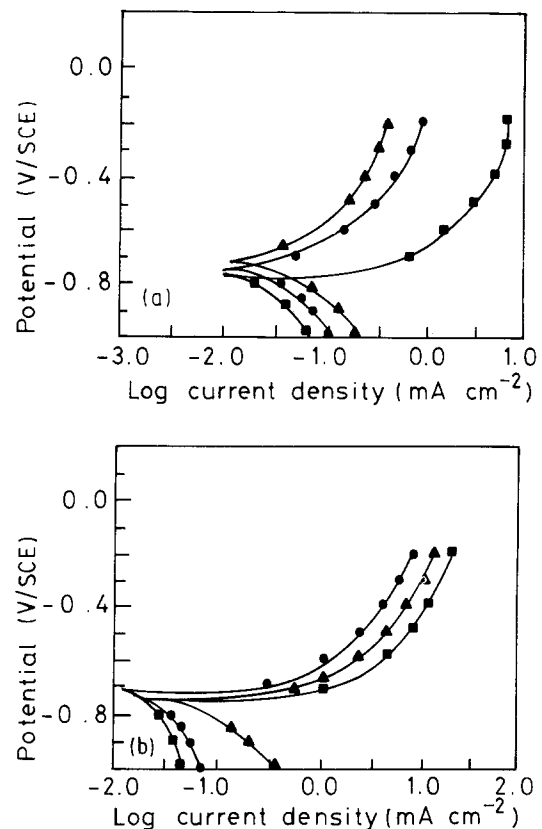


Figure 1 Potentiodynamic curves for 6061 Al alloy and 15 w/o SiC<sub>p</sub> composite in (a) sea water and (b) 3 N H<sub>2</sub>SO<sub>4</sub>. (●) 6061 Al, (▲) as-cast composite and (■) extruded composite.

at 300 K (Fig. 4a-c) also show a similar trend. Increase in concentration of acid results in enhanced attack for all the materials (Figs 5a-c to 7a-c).

### 4. Discussion

Aluminium alloys are generally passive and corrosion resistant in aqueous media except for pitting corrosion

TABLE II Composition of sea water (pH 8.10)

Constituent	Cl <sup>-</sup>	SO <sub>4</sub> <sup>2-</sup>	HCO <sub>3</sub> <sup>-</sup>	Br <sup>-</sup>	Na <sup>+</sup>	Mg <sup>2+</sup>	Ca <sup>2+</sup>	K <sup>+</sup>
Wt %	1.9	0.26	0.014	0.004	1.06	0.13	0.04	0.04

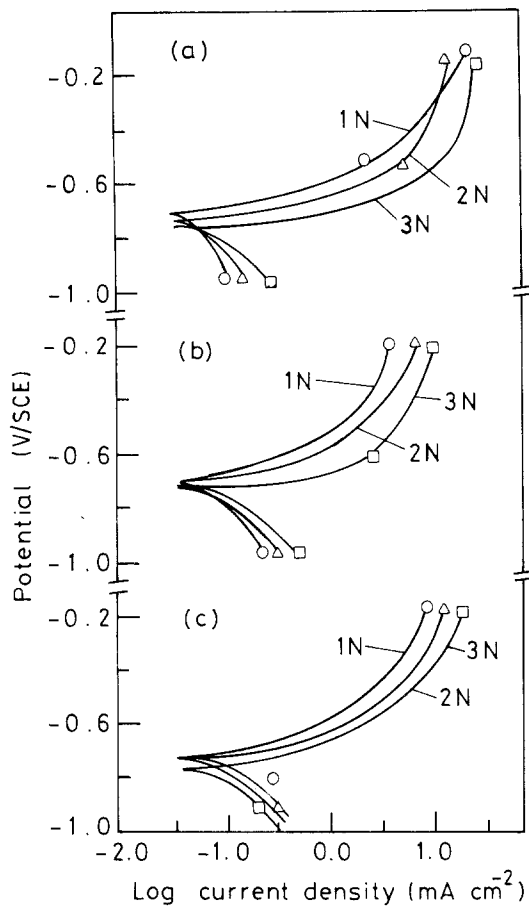


Figure 2 Potentiodynamic curves in different concentration of  $H_2SO_4$  at 325 K for (a) base alloy (6061 Al), (b) as-cast composite of 15 w/o  $SiC_p/6061$  Al and (c) extruded composite of 15 w/o  $SiC_p/6061$  Al.

due to chloride. The passive film is a poor electronic conductor and cathode reaction occurs on the micron size particles of impurity constituents or smaller precipitate particles. These determine whether the alloy will self-polarize to its pitting potential and control the rate of pitting [11]. Electrochemical measurements showed (Table IV) shifts in corrosion potential in more active direction (i.e. more negative values of potential) when  $SiC_p$  reinforcements are incorporated into Al alloys. This is an indication that the composites are more reactive and more susceptible to

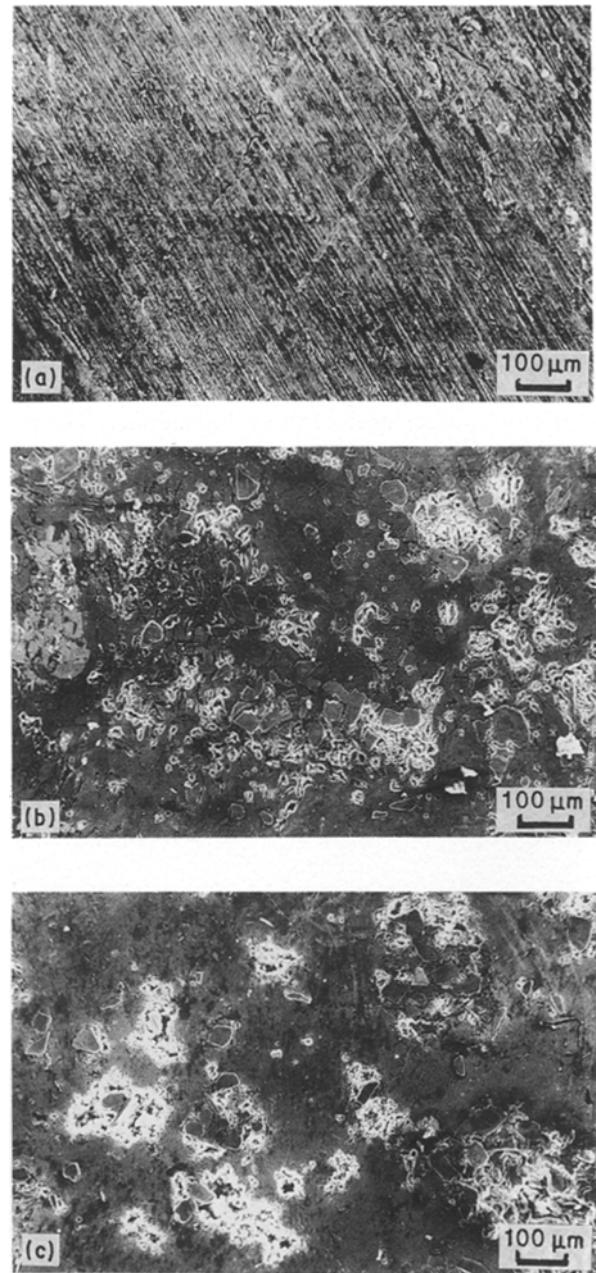


Figure 3 Scanning electron micrographs of samples corroded in sea water at 300 K ( $\times 100$ ) (a) Base alloy (6061 Al), (b) as-cast composite, and (c) extruded composite.

TABLE IV Corrosion rate of composites and base alloy in different media (Tafel extrapolation method)

Material	Sea water		1 N $H_2SO_4$		2 N $H_2SO_4$		3 N $H_2SO_4$	
	$i_{corr}$ ( $\mu A cm^{-2}$ )	Corr. rate (m.p.y.)	$i_{corr}$ ( $\mu A cm^{-2}$ )	Corr. rate (m.p.y.)	$i_{corr}$ ( $\mu A cm^{-2}$ )	Corr. rate (m.p.y.)	$i_{corr}$ ( $\mu A cm^{-2}$ )	Corr. rate (m.p.y.)
<b>A. Base alloy (6061 Al)</b>								
Temp. 300 K	17.78	7.65	19.95	8.58	100.00	43.00	116.55	50.12
325 K	10.00	4.30	12.58	5.41	79.43	34.16	39.81	17.11
<b>B. Composite (6061 Al-15 Wt% <math>SiC_p</math>)</b>								
<b>(i) As-cast</b>								
Temp. 300 K	10.30	4.43	15.85	10.79	56.20	24.18	39.89	17.12
325 K	17.78	7.65	56.23	24.18	63.09	27.13	79.43	34.15
<b>(ii) Extruded</b>								
Temp. 300 K	10.30	4.43	5.62	2.42	10.00	4.30	19.95	8.58
325 K	10.00	4.30	39.81	17.11	16.21	6.97	22.39	9.63

localized corrosion than their matrices. The corrosion current densities ( $i_{corr}$ ) as determined by Tafel extrapolation (Table IV) suggest lower corrosion rates for the composites in the extruded form. However, this anomaly can be explained on the basis of localized attack like crevice or pitting, the full extent of which may not be reflected in the  $i_{corr}$  value determined by Tafel method [12].

The reinforcing phase (SiC) or the reaction products at the interface [13] will be an effective cathode. If it is continuous, it will increase the cathode to anode ratio resulting in higher localized corrosion of the matrix. Localized corrosion at the interface can also arise due to discontinuities or fissures at the interface. The possible sources for these are decohesion or cracks of brittle interface reaction products at the interface. Besides, matrix defects too can provide continuous corrosion paths. In composites fabricated by infiltra-

tion or other solidification techniques, shrinkage porosity and impurity segregation may result in the vicinity of the reinforcements. Much of the pores can be eliminated by a hot working process such as extrusion. Further, extrusion also leads to more uniform distribution of  $SiC_p$  in the matrix.

The present results clearly show that there is uniform corrosion in the case of base alloy (6061 Al) exposed to sea water at 300 K (Fig. 3a). This form of corrosion is quite likely because of possible matrix defects such as gas porosity, impurities etc. which provide continuous corrosion paths. The 6061 Al/ $SiC_p$  composite in as-cast condition shows higher and localized attack in sea water (Fig. 3b) as expected, because of the galvanic action between the cathodic brittle interfacial layer and the matrix. The presence of agglomerates of  $SiC_p$  and pores in the matrix also enhances localised corrosion. The extruded form of

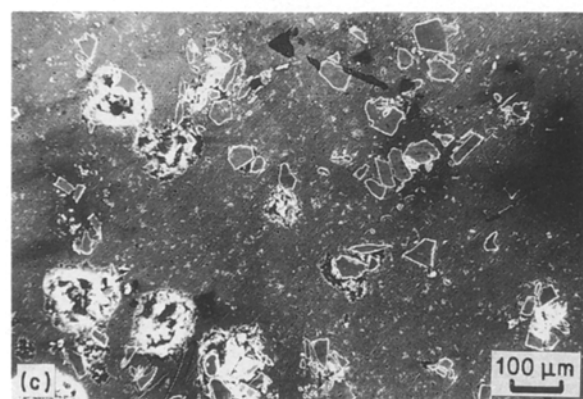
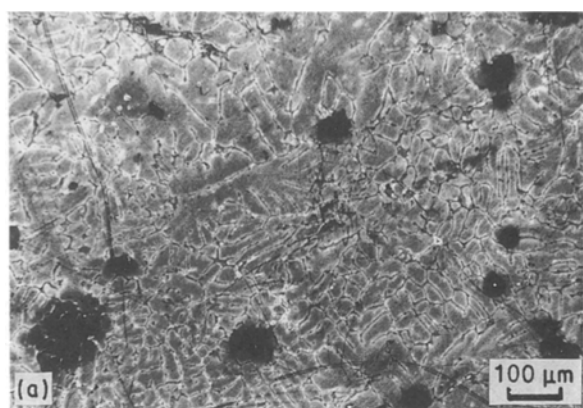


Figure 4 Micrographs of samples corroded in 3 N  $H_2SO_4$  at 300 K ( $\times 100$ ). (a) Base alloy (6061 Al), (b) as-cast composite, and (c) extruded composite.

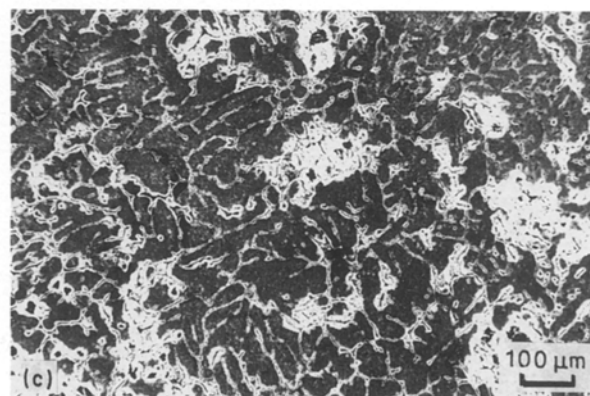
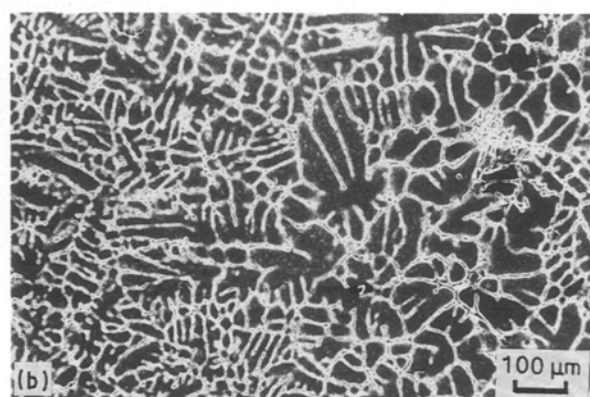
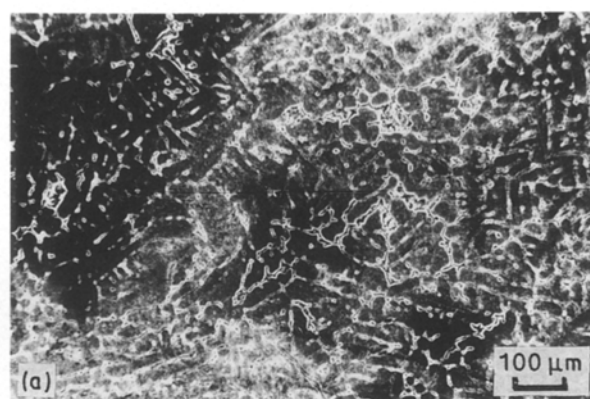


Figure 5 Micrographs of base metal corroded in acid media at 325 K ( $\times 100$ ). (a) 1 N  $H_2SO_4$ , (b) 2 N  $H_2SO_4$ , and (c) 3 N  $H_2SO_4$ .

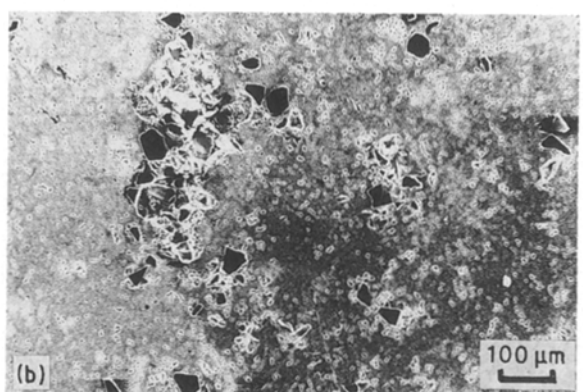
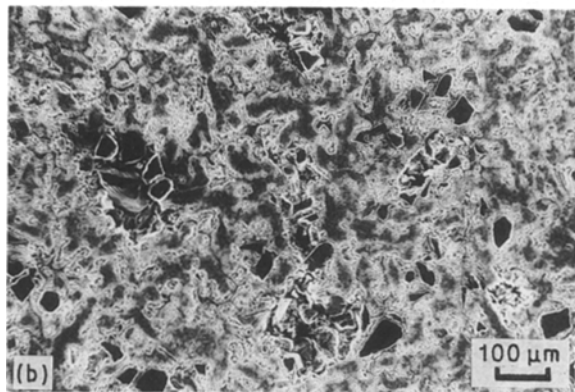
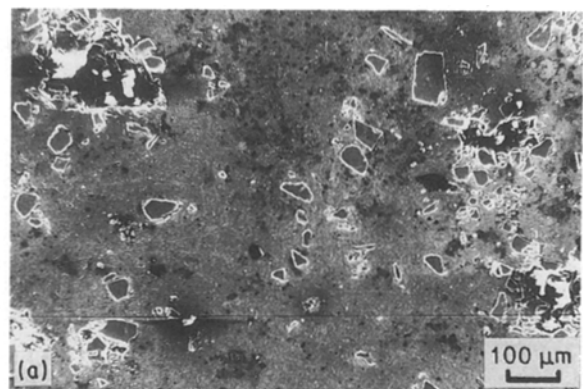
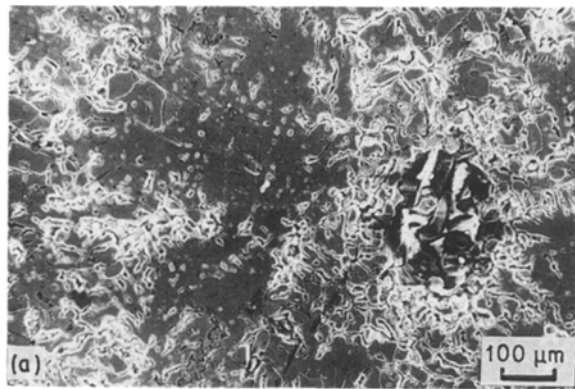


Figure 6 Micrographs of as-cast composite samples corroded at 325 K ( $\times 100$ ). (a) 1 N  $H_2SO_4$  and (b) 3 N  $H_2SO_4$ .

the composite shows lesser attack (Fig. 3c), even though localized, because of the elimination of much of the defects in the matrix and agglomerates of  $SiC_p$ . Similar behaviour is also seen in these materials when exposed to  $H_2SO_4$  medium (Fig. 4a–c). The extent of corrosion is higher in acid environment. This is due to decohesion at the interface and rupture of the more cathodic interface reaction layer resulting in the formation of localized anodic sites. The attack will be of pitting type. This can be clearly seen in Fig. 8a, b.

Increase in concentration of acid increases the corrosion of 6061 Al base alloy. The attack is generally intergranular at lower concentrations (Fig. 5a, b), while at higher concentration of acid, grains are also attacked (Fig. 5c). Besides higher dissolution rate at the grain boundaries were observed at higher concentration of acid (Fig. 8c), 6061 Al/ $SiC_p$  composite in as cast condition when exposed to acid medium shows corrosion initiation at the interface which later spreads over entire anodic region by metal (anodic) dissolution mechanism. This leads to pitting attack near the clusters or agglomerates of  $SiC$  at higher concentration of acid (Fig. 6a, c). Extruded form of composite shows less attack (Fig. 7a–c) compared to as-cast composites because of less number of voids and agglomerates of  $SiC_p$ . Electrochemical study (Fig. 2a–c) also substantiates this showing higher  $i_{corr}$  value for higher acid concentrations.

Increase of temperature invariably increases the attack, in acid medium for all the materials investigated. The increase in the attack is due to metal dissolution (anodic process) governed by the kinetics at the

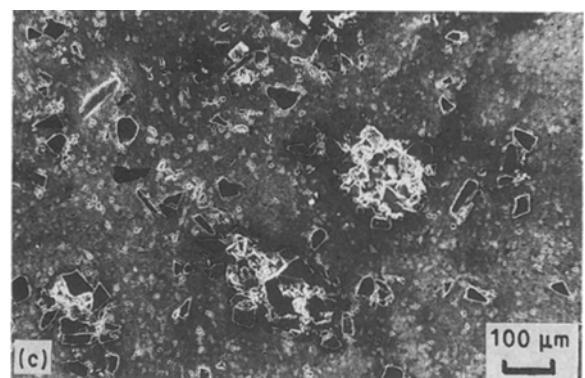


Figure 7 Micrographs of extruded samples corroded at 325 K ( $\times 100$ ). (a) 1 N  $H_2SO_4$ , (b) 2 N  $H_2SO_4$ , and (c) 3 N  $H_2SO_4$ .

temperature. This anodic process appears to be under activation control (Fig. 1b and 2a–c). SEM photo micrographs also reveal the increase in the damage with increase in temperature of the media (Fig. 4a and 5c; 4b and 6c; 4c and 7c).

## 5. Conclusions

The present study suggests that:

1. 6061 Al– $SiC_p$  composites (both as cast and extruded) exhibit more active open circuit potentials compared to the base alloy.
2. 6061 Al/ $SiC_p$  composites show localized attack both in as cast and extruded state. However, in as cast condition the extent of corrosion damage is more.
3. 6061 Al/ $SiC_p$  composites in as cast condition suffers localized corrosion in acid medium, the attack mainly confining to the interface. The corrosion rate



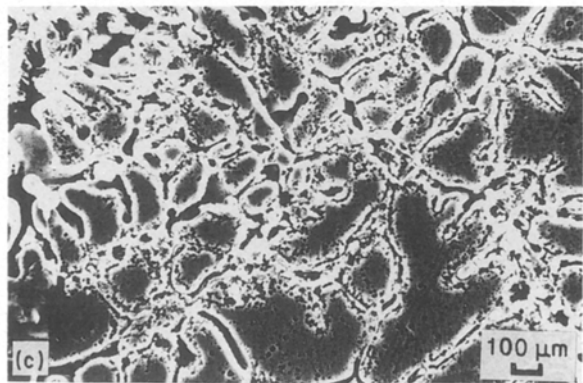
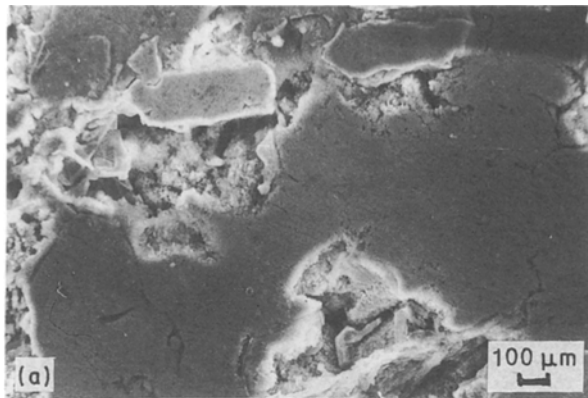


Figure 8 Micrographs of samples corroded in 3 N H<sub>2</sub>SO<sub>4</sub> ( $\times 500$ ). (a) Base alloy (6061 Al), (b) as-cast composite, and (c) extruded composite.

increases with acid concentration and temperature of the media.

4. 6061 Al/SiC<sub>p</sub> composites in the extruded state show relatively less attack compared to as cast condition, because of less defects in matrix and less agglomerates of SiC<sub>p</sub>. The increase in acid concentration and temperature increases the attack.

### Acknowledgements

The authors gratefully acknowledge the experimental support rendered by Miss H. V. Shylaja Kumari. They also thank ARDB for the financial support.

### References

1. D. M. AYLOR, "Metals Handbook", 9th edition, vol. 13, (American Society for Metals, OH 1987), p 859.
2. P. K. ROHATGI, R. ASTANA and S. DAS, *Int. Met. Rev* **31** (1986) 115.
3. A. M. PATTON, *J. Inst. Metals* **100** (1972) 197.
4. M. SAXENA, O. P. MODY, A. H. YAGNESHWARAN and P. K. ROHATGI *Corros. Sci.* **27** (1987) 249.
5. S. Z. PHOLMAN, *Corrosion* **34** (1978) 156.
6. A. J. SEDRIKS, J. A. S. GREEN and D. L. NOVAK, *Met. Trans.* **2** (1971) 871.
7. S. V. NAIR, J. K. TIEN and R. C. BATES, *Int. Met. Rev.* **30** (1985) 275.
8. DEONATH and T. K. G. NAMBOODHIRI, *Corros. Sci.* **29** (1989) 1215.
9. P. P. TRAZAKOMA, E. M. MCCAFERTY and C. R. CROWE, *J. Electrochem. Soc.* **130** (1983) 1804.
10. M. K. SURAPPA and P. K. ROHATGI, *J. Mater. Sci.* **16** (1981) 983.
11. M. METZGER and S. G. FISHMANN, *Ind. Engng. Chem. Prod. Res. Dev.* **22** (1983) 296.
12. W. H. AYLOR (Ed.), "Handbook on Corrosion Testing and Evaluation" (Wiley & Sons, New York 1971) p. 192.
13. D. J. LLOYD and I. JIN, *Met. Trans* **19A** (1988) 3107.

Received 29 June

and accepted 6 November 1990